Field structure of vortex lattices in uniaxial superconductors

Sara L. Thiemann, Z. Radović,* and V. G. Kogan†
Ames Laboratory and Physics Department of Iowa State University, Ames, Iowa 50011
(Received 27 December 1988)

The magnetic field distribution within a primitive cell of the equilibrium flux-line lattice of a uniaxial superconductor is obtained for any orientation of vortex axes within the crystal in intermediate fields. The numerical procedure is described for mapping of both longitudinal and transverse field components with respect to the vortex axes (or to the direction of the induction **B**, which is the same). For a general orientation of **B** within the crystal, the transverse field, which is comparable in value to the longitudinal one in low fields, becomes small with respect to B in intermediate fields, but remains comparable to the variable part of the longitudinal component. The nuclear magnetic resonance line shapes are discussed for an arbitrary orientation of an intermediate external field.

I. INTRODUCTION

Early indications of differences in the magnetic field distribution, $\mathbf{h}(\mathbf{r})$, within vortices of anisotropic superconductors as compared to the classical Abrikosov structure for isotropic materials can be found in the literature of the 1960's. Tilley had tried to extend his solution of the Ginzburg-Landau (GL) equations at the upper critical field H_{c2} to the field domain $(H_{c2}-H)\ll H_{c2}$.[1] The attempt was followed by Dorer and Bommel, who—to the best of our knowledge—were the first to find that $\mathbf{h}(\mathbf{r})$ must have a nonzero component transverse to the vortex axes.[2] Their solution, however, was erroneous because their *averaged* transverse field, i.e., the transverse component of the induction **B**, did not vanish. As was pointed out later by Kogan and Clem, such a component of **B** is prohibited by the flux quantization.[3] Although in that paper only the GL case $(H_{c2}-H)\ll H_{c2}$ was treated, the argument is quite general and holds at any field and temperature. Another indication for possible existence of the transverse vortex field came from the microscopic calculations of Takanaka.[4]

A clear physical picture as to the source of the transverse field arose after one of the authors (V.G.K.) pointed out that in uniaxial materials with, e.g., a large mass along the crystal axis, the persistent currents have a tendency to flow as close to the "easy" plane (with low masses) as possible.[5] The kinetic part of the free energy of the vortex-current loops is reduced when they are inclined from the plane normal to the vortex axis toward the "easy" one. This is equivalent to a nonzero component of the persistent current parallel to the vortex axis, which, in turn, results in a nonzero transverse field component. The effect, of course, vanishes if vortices are directed along one of the principal crystal directions. In more detail the problem has been considered in Ref. 3 for fields near H_{c2}. In particular, the transverse component of the macroscopic magnetization has been evaluated under the explicit condition of *zero transverse induction.* Away from H_{c2}, the London approach can be used. In this domain, existence of the transverse field follows from the London equations in a direct and simple manner, as was shown in Ref. 6 and in the later theoretical work.[7–11]

The transverse field in vortices affects the outcome of muon spin rotation (μSR) (see, e.g., Ref. 11) and nuclear magnetic resonance (NMR) experiments; the latter is discussed below. It has an influence upon the form factors of the neutron scattering from the flux lines.[12] Also, it leads to the transverse magnetization, which can be measured either directly or by observation of a torque acting on a reversible sample in intermediate fields

$$H_{c1}\ll H\ll H_{c2}\ , \tag{1}$$

where the demagnetization effects of the sample shape can be neglected.[13] The torque experiment has recently been done with the high-T_c superconductors $YBa_2Cu_3O_7$ and $Tl_2Ba_2Ca_2Cu_3O_{10}$ in the field domain (1), which is quite broad in all high-T_c materials.[14] The data are in a good agreement with predictions of Ref. 13. Thus, the transverse field in vortices of anisotropic superconductors and the transverse magnetization should be considered as experimental facts rather than theoretical speculations. This field influences the intervortex interaction, flux-line lattice structures,[12,15] and, ultimately, the vortex dynamics.

We consider in this paper the distribution $\mathbf{h}(\mathbf{r})$ in intermediate fields for an arbitrary orientation of vortices within a uniaxial crystal. Apart from an obvious interest in visualizing the complex picture of the vortex field in real space, this distribution is needed for interpretation of the NMR line shapes. In the next section we review briefly the formulas needed to reconstruct $\mathbf{h}(\mathbf{r})$. Examples of numerical results are given in Sec. III; the numerical procedure is discussed in more detail in the Appendix. The NMR line shapes and the way we evaluate them are discussed in Sec. IV. A short discussion concludes the paper.

II. LONDON EQUATIONS

Major effects of a strong uniaxial anisotropy can be taken into account by replacing the scalar $\lambda^2(\mathrm{curl}\mathbf{h})^2$ in

the London-free energy density of an isotropic material with an invariant combination $\lambda^2 m_{ik}\mathrm{curl}_i\mathbf{h}\mathrm{curl}_k\mathbf{h}$ (for details the reader may turn to Refs. 6–8). Here λ^2 is proportional to the "average mass" $M_{\mathrm{av}}=(M_1M_2M_3)^{1/3}$ with M_α being the principal values of the "mass tensor" M_{ik}. We normalize this tensor on M_{av}: $m_{ik}=M_{ik}/M_{\mathrm{av}}$; then the eigenvalues of m_{ik} are connected by $m_1m_2m_3=1$. Although m_{ik} is often called the "effective-mass tensor," it incorporates other sources of anisotropy, among which the possible gap anisotropy is most important.[16] Hereafter, we consider m_{ik} as a known phenomenological tensor. In fact, for uniaxial superconductors (in the case of our interest $m_1=m_2<m_3$) we only need to know the ratio $\Gamma=m_3/m_1$. Then the normalization $m_1{}^2m_3=1$ yields both masses: $m_1=\Gamma^{-1/3}$ and $m_3=\Gamma^{2/3}$. The anisotropy parameter Γ can be determined experimentally from, for example, the ratio of the two upper critical fields, the one directed in the basal plane ab over another one along the crystal c axis with the large mass m_3: $H_{c2,ab}/H_{c2,c}=\sqrt{m_3/m_1}=\sqrt{\Gamma}$. Another and probably better way to extract Γ is provided by the torque experiment mentioned above.[14]

The London free energy F (per unit length in the direction of vortices) now reads

$$8\pi F=\int(\mathbf{h}^2+\lambda^2 m_{ik}\mathrm{curl}_i\mathbf{h}\mathrm{curl}_k\mathbf{h})dx\,dy\ , \tag{2}$$

where $\mathbf{h}(x,y)$ is the local magnetic field and $dx\,dy$ is an element of area in the plane normal to the direction $\hat{\mathbf{z}}$ of vortex axes. For a vortex along $\hat{\mathbf{z}}$, the field $\mathbf{h}$ in an anisotropic material has h_x and h_y nonzero components, unless the vortex axis coincides with one of the principal crystal directions.[6]

We wish to consider vortices oriented arbitrarily with respect to the crystal frame (X,Y,Z) defined in Fig. 1, and, therefore, we transform m_{ik} from the crystal frame (where $m_{XX}=m_{YY}=m_1$ and $m_{ZZ}=m_3$) to the "vortex frame" (x,y,z):

$$\begin{aligned}&m_{xx}=m_1\cos^2\theta+m_3\sin^2\theta,\quad m_{xy}=m_{yz}=0\ ,\\&m_{yy}=m_1,\quad m_{zz}=m_1\sin^2\theta+m_3\cos^2\theta\ ,\\&m_{xz}=(m_1-m_3)\sin\theta\cos\theta\ ,\end{aligned} \tag{3}$$

where θ is the angle between $\hat{\mathbf{c}}$ or $(\hat{\mathbf{Z}})$ and the vortex axes $\hat{\mathbf{z}}$ (or $\mathbf{B}$). The London equations for a lattice of vortices located at $\mathbf{r}_\nu$ are obtained by varying F with respect to $\mathbf{h}(x,y)$:

$$\begin{aligned}&h_x-\lambda^2(m_{zz}h_{x;\alpha\alpha}-m_{xz}h_{z;yy})=0\ ,\\&h_y-\lambda^2(m_{zz}h_{y;\alpha\alpha}+m_{xz}h_{z;xy})=0\ ,\\&h_z-\lambda^2(m_1h_{z;xx}+m_{xx}h_{z;yy}-m_{xz}h_{x;\alpha\alpha})=\Phi_0\sum_\nu\delta(\mathbf{r}-\mathbf{r}_\nu)\ .\end{aligned} \tag{4}$$

Here, e.g., $h_{i;xy}=\partial^2h_i/\partial x\,\partial y$, $h_{i;\alpha\alpha}$ means the two-dimensional Laplacian in the xy plane, and $\mathbf{r}=(x,y)$ and $\mathbf{r}_\nu$ form a two-dimensional periodic lattice in the xy plane. Furthermore, Φ_0 is the flux quantum, so that the magnetic induction $B=\Phi_0/S$ with S being the primitive cell area. Note that in the system of straight vortices parallel to $\hat{\mathbf{z}}$, nothing depends upon z. The field $\mathbf{h}(\mathbf{r})$ has

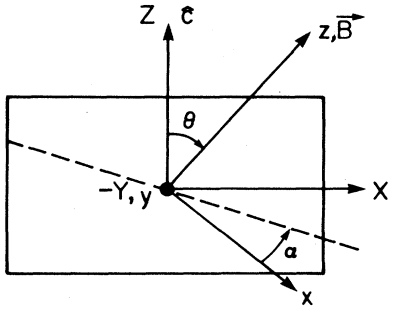

FIG. 1. The system of coordinates (x,y,z) with $\mathbf{z}=\mathbf{B}/B$ is obtained by rotation θ of the crystal frame (X,Y,Z) about the Y axis. The plane in which the currents flow is defined by the y axis and the dashed line (see Sec. III).

the periodicity of the vortex lattice, so that it can be expanded in the Fourier series:

$$\mathbf{h}(\mathbf{r})=\sum_{\mathbf{G}}\mathbf{h}(\mathbf{G})\exp(i\mathbf{G}\cdot\mathbf{r})\ , \tag{5}$$

$$\mathbf{h}(\mathbf{G})=(B/\Phi_0)\int\mathbf{h}(\mathbf{r})\exp(-i\mathbf{G}\cdot\mathbf{r})d^2\mathbf{r}\ , \tag{6}$$

where $\mathbf{G}$ forms a reciprocal lattice and the integral in Eq. (6) is extended over the cell area. Equations (4) now yield for $\mathbf{h}(\mathbf{G})$:

$$h_x(\mathbf{G})=B\lambda^2m_{xz}G_y{}^2/d\ , \tag{7a}$$

$$h_y(\mathbf{G})=-B\lambda^2m_{xz}G_xG_y/d\ , \tag{7b}$$

$$h_z(\mathbf{G})=B(1+\lambda^2m_{zz}G^2)/d\ , \tag{7c}$$

$$d=(1+\lambda^2m_1G_x{}^2+\lambda^2m_{xx}G_y{}^2)(1+\lambda^2m_{zz}G^2)-\lambda^2m_{xz}G^2G_y{}^2\ . \tag{7d}$$

The equilibrium lattice structure for an arbitrary orientation of $\mathbf{B}$ (which coincides with the direction of vortex axes) has been obtained in Refs. 12 and 15 for intermediate fields (1).[17] The basis vectors, $\mathbf{b}_{1,2}$, of the primitive cell are

$$\begin{aligned}\mathbf{b}_1&=\left[\frac{2\Phi_0}{B}\right]^{1/2}\left[\frac{m_{zz}}{3m_3}\right]^{1/4}\hat{\mathbf{x}}\ ,\\\mathbf{b}_2&=\frac{b_1}{2}\left[\hat{\mathbf{x}}+\left[\frac{3m_3}{m_{zz}}\right]^{1/2}\hat{\mathbf{y}}\right]\ .\end{aligned} \tag{8}$$

The lattice consists of isosceles triangles (Fig. 2) with the side-to-base ratio b_2/b_1 and the angle ϕ between $\mathbf{b}_1$ and $\mathbf{b}_2$ given by

$$2b_2/b_1=(1+3m_3/m_{zz})^{1/2},\quad\tan\phi=(3m_3/m_{zz})^{1/2}\ . \tag{9}$$

The triangles become equilateral for the field $\mathbf{B}$ parallel to $\hat{\mathbf{c}}$ $(\theta=0)$, where $m_{zz}=m_3$, as they should. It is worth noting that the equilibrium lattice (8) of vortices in a uniaxial material is attached to the crystal in a unique way. Unlike the isotropic case, any rotation of the cell (8) as a whole around the direction of $\mathbf{B}$ ($\hat{\mathbf{z}}$ axis) would have in-

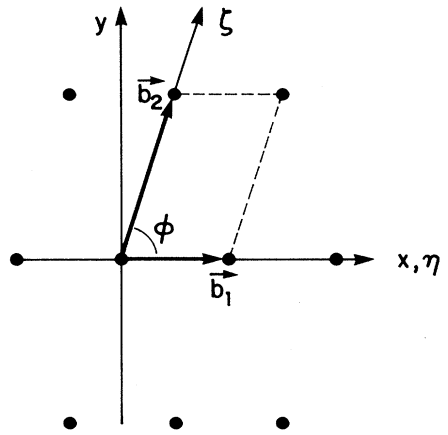

FIG. 2. Sketch of the equilibrium lattice cell [given in Eqs. (8) and (9)] in the plane (x,y) normal to **B**. The nonorthogonal coordinates (ζ,η) are introduced in the Appendix to simplify the numerical procedure.

creased the free energy. The directions $\hat{\mathbf{x}}$ and $\hat{\mathbf{y}}$ can be written as $(\mathbf{c}\times\mathbf{B})\times\mathbf{B}/B^2$ and $\mathbf{c}\times\mathbf{B}/B$, respectively.

The reciprocal lattice corresponding to the cell (8) is found readily:

$$G_x=\pi\left[\frac{2B}{\Phi_0}\right]^{1/2}\left[\frac{3m_3}{m_{zz}}\right]^{1/4}n\ ,$$
$$G_y=\pi\left[\frac{2B}{\Phi_0}\right]^{1/2}\left[\frac{m_{zz}}{3m_3}\right]^{1/4}(2m-n)\ , \tag{10}$$
$$m,n=0,\pm1,\pm2,\cdots\ .$$

We now have all the information necessary to recover the field distribution $\mathbf{h}(\mathbf{r})$ with the help of the Fourier transform (5).

III. FIELD DISTRIBUTION

The details of the numerical procedure used are given in the Appendix. To present the results we have chosen the mass ratio $\Gamma=m_3/m_1=25$, the figure which is believed currently to reflect the anisotropy of the high-T_c superconductor $YBa_2Cu_3O_{7-\delta}$ with $T_c\sim90$ K; see, e.g., Ref. 14. (Recall that due to the normalization, $m_1^2m_3=1$, both reduced masses are expressed in terms of their ratio: $m_1=\Gamma^{-1/3}$, $m_3=\Gamma^{2/3}$.) The average penetration depth λ of all known high-T_c materials is about 100 times larger than their average coherence length ξ; then, roughly, the GL parameter $\kappa=\lambda/\xi\simeq10^2$. The low critical field $H_{c1}=(\Phi_0/4\pi\lambda^2)\sqrt{m_{zz}}\ln\kappa$ or, taking Φ_0/λ^2 as the unit of field, $H_{c1}=(\sqrt{m_{zz}}\ln\kappa)/4\pi$. We take for a representative example $B=2$. This B exceeds substantially the H_{c1} in the most interesting part of the interval $0<\theta<\pi/2$ [for $\mathbf{B}\|\mathbf{c}$ $(\theta=0)$, $\sqrt{m_{zz}}=\sqrt{m_3}\simeq2.9$ and $B/H_{c1}(0)\simeq1.9$, while for $\mathbf{B}\perp\mathbf{c}$ $(\theta=\pi/2)$, $\sqrt{m_{zz}}=\sqrt{m_1}\simeq0.58$ and $B/H_{c1}(\pi/2)\simeq9.3$]. Figure 3 maps the distribution of the longitudinal component $h_z(x,y)$ for three orientations of **B** (or of the vortex axes) with respect to the c axis: $\theta=0°$, 70°, and 90°. The contours of constant $h_z(x,y)$ are shown starting with a value of h_z close to B (to avoid the domain with high field gradients) spaced at intervals of Δh_z (see the figure caption). These same lines also represent the stream lines of the current density projection upon the xy plane.

For the graphic representation of the transverse field $\mathbf{h}_{tr}(\mathbf{r})$, we notice that both h_x and h_y are expressed in terms of the z component of the vector potential **A**: $h_x=\partial A_z/\partial y$, $h_y=-\partial A_z/\partial x$. For an element dl of the $\mathbf{h}_{tr}$ streamline we have

$$0=(dl\times\mathbf{h}_{tr})_z=h_y dx-h_x dy=-dA_z\ .$$

The streamlines of $\mathbf{h}_{tr}$ are, therefore, given by $A_z(x,y)=$const. For this reason we Fourier-transform the function

$$A_z(\mathbf{G})=ih_y(\mathbf{G})/G_x=h_x(\mathbf{G})/iG_y=-iBm_{xz}G_y/d \tag{11}$$

[see Eqs. (7)] to find $A_z(\mathbf{r})$ and plot the contours $A_z(x,y)=$const. Due to the factor m_{xz}, the transverse field vanishes if **B** points in one of the principal crystal directions. The lines of $\mathbf{h}_{tr}$ are shown in Fig. 4 for $\theta=70°$ and $B=2$, corresponding to the graph in Fig. 3(b); the values and directions of $\mathbf{h}_{tr}$ are extracted from the numerical data on $h_x(\mathbf{r})$ and $h_y(\mathbf{r})$. It is clear from the figure that the total magnetic flux in both the x and y directions is zero, as it must be.[3] We have checked that this condition is satisfied by direct numerical summation of the results for both h_x and h_y over the primitive cell.

One can see from Fig. 4 that the transverse field is maximum at vortex axes, i.e., the total field at vortex axes is *not parallel* to the direction of the axes (or to **B**) (the latter is normal to the figure plane). The deviation of the **h** direction from that of **B** depends on the position within the cell; Fig. 4 shows that it changes sign twice as one moves along the line $x=0$, e.g., from the "cell bottom" at $y=0$ to the "top" at $y=b_2\sin\phi$. The strips where h_x has different signs are separated by domains where "vorticity" of the field lines develops; in these domains the total field has a helical structure streaming up along **B** (with helicities of different signs in different parts of the cell).

An important characteristic of the field distribution is the root-mean-square deviation from **B**:

$$\langle(\mathbf{h}-\mathbf{B})^2\rangle=\sum_{\mathbf{G}}{}'h^2(\mathbf{G})=\frac{B^2}{m_1^2\lambda^4}\sum_{\mathbf{G}}{}'G^2\frac{m_{xz}^2G_y^2+m_{zz}^2G^2}{(m_{zz}G_x^2+m_3G_y^2)^2}\ , \tag{12}$$

where the sum runs over the reciprocal lattice (10) except for the origin $\mathbf{G}=\mathbf{0}$. [To avoid misunderstanding, note the difference between the variance of the vector **h**, defined in Eq. (12), and the variance $\langle(h-B)^2\rangle$ for the field value.] In substituting the Fourier components $h_i(\mathbf{G})$ of Eqs. (7) in Eq. (12), we had neglected 1's with

respect to terms $\lambda^2 G^2 \gg 1$, a good approximation in intermediate fields (1). The expression under the sum (12) is of the order G^{-4}, and the sum is well convergent. As is seen from Eqs. (10), $G^4 \propto B^2$; hence, the factor B^2 drops off the right-hand side of (12). In other words, in intermediate fields the field variance is *field independent*, the result known for isotropic materials.[18]

After a straightforward algebra one obtains

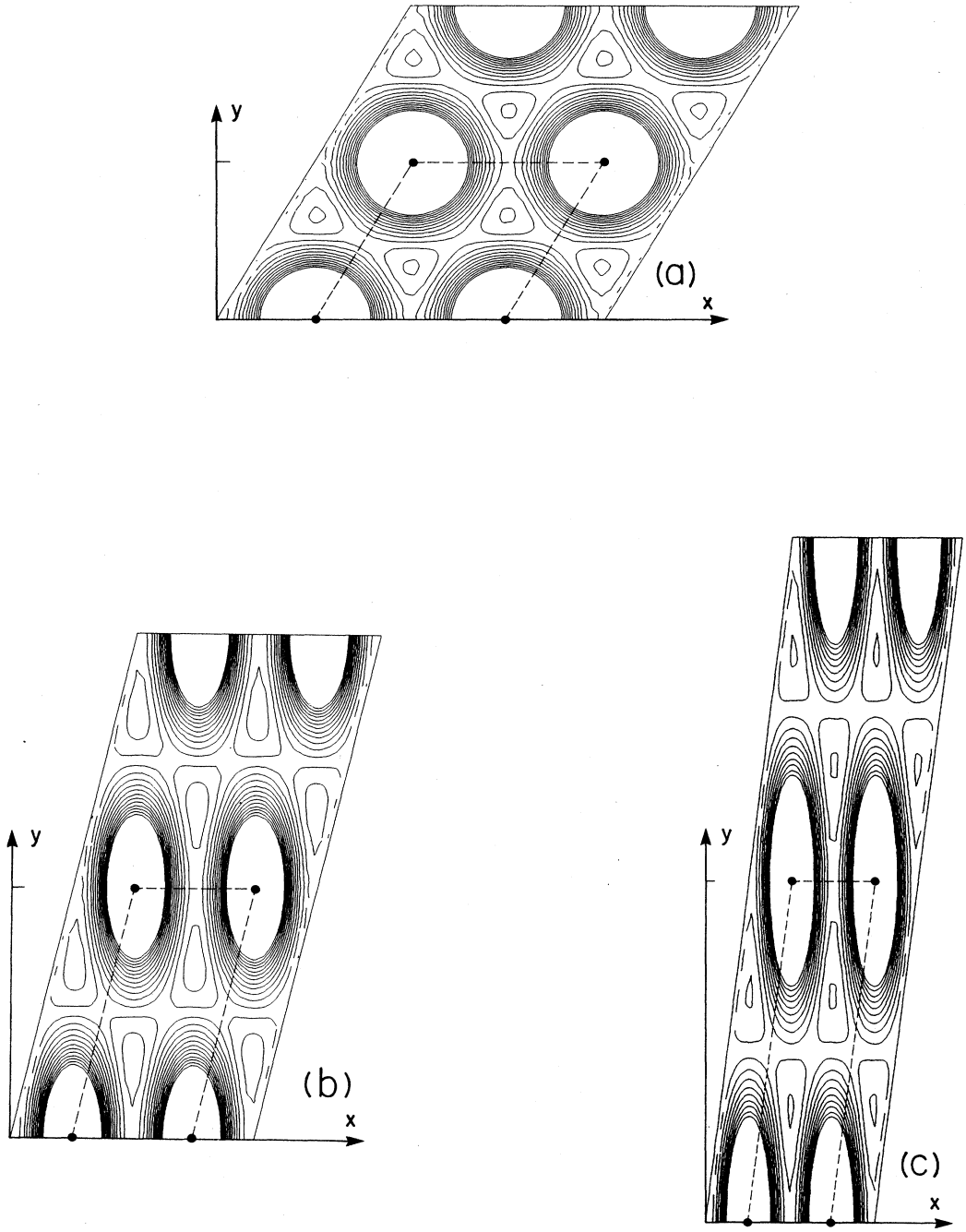

FIG. 3. Contours of constant axial field $h_z(x,y)$ for three orientations θ of **B** with respect to the c axis for the same value of $B=2.0$ in units of Φ_0/λ^2 and $m_3/m_1=25$. The contours are plotted starting with an initial value h_{in} and decreasing at intervals Δh_z: (a) $h_{in}=1.999$, $\Delta h_z=-0.010$, (b) $h_{in}=2.020$, $\Delta h_z=-0.005$, and (c) $h_{in}=2.005$, $\Delta h_z=-0.003$. Contours close to the vortex axes are omitted; the field gradients are too large there and the contours would not have been resolved.

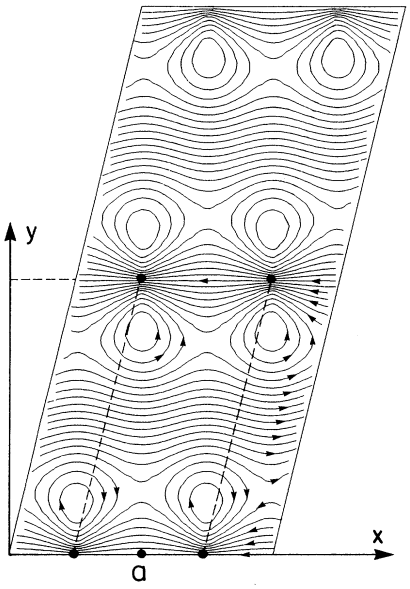

FIG. 4. The lines of the transverse field $\mathbf{h}_{tr}$ for $\mathbf{B}$ at angle $\theta=70°$ to $\mathbf{c}$ for $B=2\Phi_0/\lambda^2$. A representative value of h_{tr} at the point a of the figure is 0.087.

$$\langle(\mathbf{h}-\mathbf{B})^2\rangle=\frac{3\Phi_0^2 m_{zz}}{64\pi^4\lambda^4}\sum_{m,n}{}'\frac{1+(m_{xz}/m_{zz})^2 f(m,n;\eta)}{(m^2-mn+n^2)^2}\ , \tag{13}$$

where

$$f=\frac{m^2-mn+n^2/4}{m^2-mn+n^2(1+\eta)/4},\quad \eta=\frac{3m_3}{m_{zz}}\ .$$

The summation in Eq. (13) is done numerically; the result for $\langle(\mathbf{h}-\mathbf{B})^2\rangle$ in units of Φ_0^2/λ^4 is shown in Fig. 5 for $\Gamma=25$. For a given field in the domain (1), the width of the variable part of the field distribution decreases with θ; it is maximum at $\theta=0$, decreases as θ grows, and reaches the minimum at 90°. The ratio of the maximum to the minimum is Γ, e.g., 25 in our example.

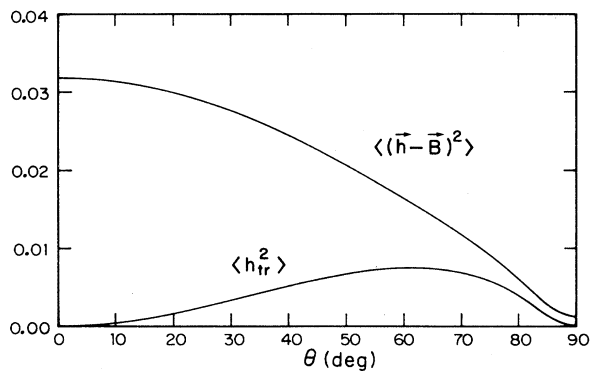

FIG. 5. The variance $\langle(\mathbf{h}-\mathbf{B})^2\rangle$ (upper curve) and $\langle\mathbf{h}_{tr}^2\rangle$ (lower curve) in units of $(\Phi_0/\lambda^2)^2$ vs the angle θ between $\mathbf{B}$ and $\mathbf{c}$ for $B=2(\Phi_0/\lambda^2)$.

In the same manner, one can evaluate the average square of the transverse field,

$$\langle h_{tr}^2\rangle=\sum_{\mathbf{G}}{}'[h_x^2(\mathbf{G})+h_y^2(\mathbf{G})]\ , \tag{14}$$

which is given by Eq. (13) without "1" in the numerator under the sum. This is shown in Fig. 5 for the same anisotropy parameter $\Gamma=25$. Thus, the transverse field scales with the *variation of the total field,* unless θ is close to 0° or 90°. Similar to the variance of $\mathbf{h}$, the mean square of the transverse field is independent of B in intermediate fields. However, its relative value, $\langle h_{tr}^2\rangle/B^2$, decreases, and directional deviations of $\mathbf{h}$ from $\mathbf{B}$ become smaller in increasing fields.

It is worth mentioning that for well separated vortices, unlike the situation in intermediate fields, the transverse and axial fields are of the same order of magnitude.[6] Hence, the relative effect of the transverse field is greater in low fields near H_{c1} [unfortunately, only the asymptotic behavior of $\mathbf{h}(\mathbf{r})$ for $r\gg\lambda$ has been studied for an isolated vortex; as well, little is known about the equilibrium structure of the flux-line lattice in low fields[17]]. Nevertheless, in phenomena related only to the field *variation*, such as μSR, NMR, or macroscopic magnetization,[19] $\mathbf{h}_{tr}$ cannot be neglected in any field up to H_{c2}.[3]

In intermediate fields the average intervortex distance L is small compared to the average value of λ. This means that the derivatives $h_{i;\alpha\beta}\sim h_i/L^2\gg h_i/\lambda^2$, and, therefore, one can disregard the first terms in the London equations (4). The first of Eqs. (4) then reads $0=m_{zz}h_{x;\alpha\alpha}-m_{xz}h_{z;yy}$. Using $\mathrm{div}\mathbf{h}=0$ and $\partial/\partial z=0$, one obtains

$$m_{zz}(h_{x;yy}-h_{y;yx})-m_{xz}h_{z;yy}=-(m_{zz}j_z+m_{xz}j_x)_{;y}=0$$

(the factor $4\pi/c$ is omitted). The second of Eqs. (4) results in $(m_{zz}j_z+m_{xz}j_x)_{;x}=0$. Hence, the combination $m_{zz}j_z+m_{xz}j_x$ is a constant which must be zero, because the integrals of both j_x and j_z over the cell must vanish.

$$m_{zz}j_z+m_{xz}j_x=0\ . \tag{15}$$

This result has a simple meaning: In fields $H\gg H_{c1}$, the current flows in the plane that is obtained by rotation α of the xy plane about the y axis such that

$$\tan\alpha=-m_{xz}/m_{zz}\ . \tag{16}$$

In other words, though all the currents are situated in a plane, the plane is not perpendicular to the vortex axes. This plane is shown by the dashed line in Fig. 1. We derived the result given in Eqs. (15) and (16) for intermediate fields (1); in fact, it holds also near H_{c2}.[5,3]

In conclusion of this section, we note that ours is not the first attempt to plot the transverse field; for weakly anisotropic material ($m_3/m_1\simeq1$), this was done by Krzyszton and Wrobel.[10] Schopohl and Baratoff[9] used the asymptotic result at large (with respect to λ) distances from the vortex core to plot the transverse field of a single vortex.

IV. NMR LINE SHAPES

The shape of the NMR absorption versus frequency of the ac field is directly related to the distribution of $|\mathbf{h}|$ in the primitive cell of the flux line lattice.[18,20] Clearly, the absorption intensity in a given small frequency interval, $\delta\omega$, is proportional to the fraction of the cell area where the field value is in a corresponding interval ($\delta\omega \propto \delta h$). Having obtained the distribution of $\mathbf{h}(\mathbf{r})$ in the form of a discrete matrix with certain coordinates (x,y) assigned to all elements, one can easily find approximate line shapes by direct count of the relative number of (x,y) points for which the field value is between h and $h+\delta h$.

Figure 6 shows the result of such a count plotted versus parameter $f=(h-h_{\min})/(B-h_{\min})$ for $B=2(\Phi_0/\lambda^2)$, $\Gamma=25$, and for three orientations of $\mathbf{B}$ within the crystal: $\theta=0°$, 70°, and 90°. Note that $f=1$ corresponds to $h=B$. Because the curves decrease monotonically for $h>B$, these parts are not shown in the figure. Two features are worth noting. The extra saddle point of $h(\mathbf{r})$ is evident in the line shape as an extra maximum in Fig. 6 for 70°. The relative position of the main maximum (corresponding to the saddle which does not disappear at $\theta=0$) changes with the angle θ; it moves to higher fields as θ increases from 0° to about 70°, after which it falls to its initial ($\theta=0$) value at 90°.

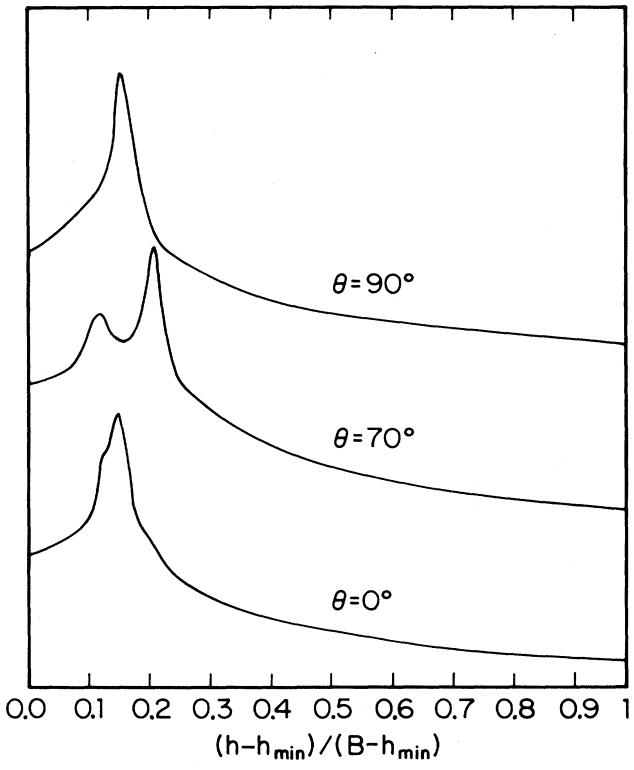

FIG. 6. Approximate NMR line shapes for $B=2(\Phi_0/\lambda^2)$ and $\theta=0°$, 70°, and 90°. The vertical units are arbitrary; the curves are displayed vertically to avoid overlap.

V. DISCUSSION

The main motivation for this work was to demonstrate substantial differences in the field distribution within vortices of anisotropic superconductors as compared to their isotropic counterparts. The vortices are the elementary entities of the macroscopic mixed state of superconductors; any changes in their magnetic structure translate into qualitatively new features of the macroscopic magnetic behavior.

The most profound manifestation of the transverse field in vortices is the transverse magnetization, which has recently been observed in the torque experiments.[14] This, of course, does not exhaust all possible implications of the peculiar magnetic structure of the mixed phase in anisotropic superconductors. The list of these implications is not yet completed. However, it is already clear that one cannot properly interpret experiments such as μSR, NMR, or the neutron scattering without explicitly taking the transverse field into account (or implicitly, in the specific form of the Fourier components of the field). We name some other phenomena where the details of the vortex magnetic structure are of importance: Elastic properties of the flux-line lattices in anisotropic superconductors[21] affect in an essential way the pinning characteristics of anisotropic materials with implications on the vast and still poorly understood domain of critical currents in strongly anisotropic high-T_c superconductors. The low-field vortex dynamics, in particular, should be more complicated than that of the isotropic case, because the transverse field in this domain is of the same order as the axial one.[6]

ACKNOWLEDGMENTS

The authors appreciate useful discussions with Professor J. R. Clem, and the support of the Solid State Group of the Ames Laboratory they enjoyed in the course of this work. Ames Laboratory is operated for the U.S. Department of Energy (USDOE) by Iowa State University under Contract No. W-7405-Eng-82. This work was supported by the Director for Energy Research, Office of Basic Energy Sciences of USDOE and, in part, by the National Science Foundation (NSF) Division of International Programs, Grant No. INT-8509361 for the U.S.-Yugoslavia scientific cooperation.

APPENDIX

For the numerical work it is convenient to use λ as the unit of length and Φ_0/λ^2 as the unit of field. Keeping the same notation for the new dimensionless quantities, we replace $\mathbf{h}\rightarrow\mathbf{h}\lambda^2/\Phi_0$, $\mathbf{B}\rightarrow\mathbf{B}\lambda^2/\Phi_0$, $\mathbf{r}\rightarrow\mathbf{r}/\lambda$, and $\mathbf{G}\rightarrow\mathbf{G}\lambda$. This results in Eqs. (7) with all λ^2 omitted, and in Eqs. (8) and (10) with omitted Φ_0. For given input parameters B, θ, and m_3/m_1, Eqs. (9) along with $b_1 b_2 \sin\phi = 1/B$ yield the parameters of the primitive cell: b_1, b_2, and ϕ.

Standard routines for the fast Fourier transform are designed for two-dimensional periodic functions defined on a square lattice. To make use of this feature, we first introduce the nonorthogonal coordinates η and ζ shown in Fig. 1:

$$\eta = x - y\cot\phi, \quad \zeta = y/\sin\phi \ . \tag{A1}$$

In these coordinates $\mathbf{h}(\eta + nb_1, \zeta + mb_2) = \mathbf{h}(\eta,\zeta)$ with integers n and m. Then we have, instead of Eqs. (5) and (6),

$$\mathbf{h}(\eta,\zeta) = \sum_{n,m} \mathbf{h}(p,q) e^{i(p\eta + q\zeta)} \ , \tag{A2}$$

$$\mathbf{h}(p,q) = B \int d\eta\, d\zeta\, \mathbf{h}(\eta,\zeta) e^{-i(p\eta + q\zeta)} \ , \tag{A3}$$

where $p = 2\pi n/b_1$ and $q = 2\pi m/b_2$ run from $-\infty$ to $+\infty$. The integral in (A3) is extended over the rectangular cell $0 \geq \eta \geq b_1$, $0 \geq \zeta \geq b_2$. Executing the transformation (A1) in Eqs. (4) for $\mathbf{h}(\mathbf{r})$ and using Eq. (A3), one obtains for the Fourier components $\mathbf{h}(p,q)$

$$h_x = h_y F_1/F_3 = h_z m_{xz} F_1/(1 + m_{zz}F_2) \ , \tag{A4}$$

$$h_z = B\left[1 + m_1 p^2 + F_1 \frac{m_{xx} + m_1 m_3 F_2}{1 + m_{zz}F_2}\right] \ , \tag{A5}$$

where

$$\begin{aligned} F_1 &= (p^2\cos^2\phi + q^2 - 2pq\cos\phi)/\sin^2\phi \ , \\ F_2 &= (p^2 + q^2 - 2pq\cos\phi)/\sin^2\phi \ , \\ F_3 &= (p^2\cos\phi - pq)/\sin\phi \ . \end{aligned} \tag{A6}$$

---

*Permanent address: Institute of Physics, Belgrade, Yugoslavia.
†Current address: Theoretical Physics Institute, Physics Department, University of Minnesota, Minneapolis, MN 55455.

[1]D. R. Tilley, Proc. Phys. Soc. London **85**, 1177 (1965).
[2]G. L. Dorer and H. E. Bommel, Phys. Rev. **183**, 528 (1969).
[3]V. G. Kogan and J. R. Clem, Phys. Rev. B **24**, 2497 (1981).
[4]K. Takanaka, Phys. Status Solidi (B) **68**, 623 (1975).
[5]V. G. Kogan, Physica **107B**, 303 (1981).
[6]V. G. Kogan, Phys. Rev. B **24**, 1572 (1981).
[7]A. M. Grishin, Fiz. Nizk. Temp. **9**, 277 (1983) [Sov. J. Low Temp. Phys. **9**, 138, (1983)].
[8]A. V. Balatskii, L. I. Burlachkov, and L. P. Gor'kov, Zh. Eksp. Teor. Fiz. **90**, 1478 (1986) [Sov. Phys.—JETP **63**, 866 (1986)].
[9]N. Schopohl and A. Baratoff, Physica C **153-155**, 689 (1988).
[10]T. Krzyszton and P. Wrobel, Phys. Status Solidi B **K41**, 144 (1988).
[11]W. Barford and J. M. F. Gunn, Physica C **156**, 515 (1988).
[12]V. G. Kogan, Phys. Lett. **85A**, 298 (1981).
[13]V. G. Kogan, Phys. Rev. B **38**, 7049 (1988).
[14]D. E. Farrell, C. M. Williams, S. A. Wolf, N. P. Bansal, and V. G. Kogan, Phys. Rev. Lett. **61**, 2805 (1988).
[15]L. J. Campbell, M. M. Doria, and V. G. Kogan, Phys. Rev. B **38**, 2439 (1988).
[16]L. P. Gor'kov and T. K. Melik-Barkhudarov, Zh. Eksp. Teor. Fiz. **45**, 1493 (1963) [Sov. Phys.—JETP **18**, 1031 (1964)].
[17]The question of the equilibrium vortex-lattice structure in low fields, $H \sim H_{c1}$, is still debated. The authors of Ref. 9 (private communication) obtained a structure different from that given in Ref. 8.
[18]E. H. Brandt, Phys. Rev. B **37**, 2349 (1988).
[19]V. G. Kogan, M. M. Fang, and Sreeparna Mitra, Phys. Rev. B **38**, 11 958 (1988).
[20]A. G. Redfield, Phys. Rev. B **162**, 367 (1967).
[21]V. G. Kogan and L. J. Campbell, Phys. Rev. Lett. **62**, 1552 (1989).